Phys. Status Solidi A **207**, No. 1, 49–66 (2010) / **DOI** 10.1002/pssa.200925148

physica status solidi a
www.pss-a.com
applications and materials science

Feature Article

Enrichment of silicon for a better kilogram

P. Becker*[,1], H.-J. Pohl[2], H. Riemann[3], and N. Abrosimov[3]

[1] Physikalisch-Technische Bundesanstalt, Bundesallee 100, 38116 Braunschweig, Germany
[2] VITCON – Projectconsult, Jena, Germany
[3] Institut für Kristallzüchtung, Berlin, Germany

Received 1 April 2009, revised 10 August 2009, accepted 12 August 2009
Published online 1 October 2010

PACS 06.20.Jr, 06.30.Dr, 61.72.uf, 68.65.−k, 81.05.Cy, 81.10.−h

* Corresponding author: e-mail peter.becker@ptb.de, Phone: +49 531 5924300, Fax: +49 531 5924305

A metrological challenge is currently underway to replace the present definition of the kilogram by the mass of a certain number of silicon atoms. A prerequisite for this is that the Avogadro constant, N_A, which defines the number of atoms in a mole, is determined with a relative uncertainty of better than 2×10^{-8}. Silicon crystals are used for this determination, the difficulty arising thereby is the measurement of the average molar mass of natural Si. Consequently, a worldwide collaboration has been launched to produce ∼5 kg of ^{28}Si single crystal with an enrichment factor greater than 0.99985 and of sufficient chemical purity so that it can be used to determine N_A with the targeted relative measurement uncertainty mentioned above. In the following, the development and first successful tests of all technological steps are reported, and the new equipment for the production of high-purity ^{28}Si with an enrichment of not less than 0.9999 is described. All steps are defined by a Technical Road Map (TRM28) mandatory for all partners, and all key results are measured by calibrated and certified means, *e.g.* the C content of the final material is less than 10^{15} atoms/cm^3 and the specific resistance is in the range from 400 to 1000 Ωcm. New applications based on this highly enriched and purified ^{28}Si, and on ^{29}Si and ^{30}Si monocrystals produced in parallel, are reported briefly in the fields of solid state spectroscopy, spintronics, quantum computing, cooling of highly loaded SYS optics, superlattice structure (SLS), terahertz laser.

1 Introduction The Avogadro constant is a remarkable feature of our physical–chemical model of nature: it relates to fundamental constants, it serves as the unit for amount-of-substance measurements and its numerical value serves as a scaling factor between quantities measured on the macroscopic scale and the same quantities on the atomic scale. The concept of an 'Avogadro constant' results from our perception of a 'particulate' nature of matter and the ensuing concept of 'numeracy' of entities in chemistry and physics. Its potential of being combined with this other allocated property of material which is 'mass', makes it very important for physicists. The combination of the properties numeracy and mass opens the possibility of defining the unit for mass, the kilogram, in a very understandable way as the mass of a defined number of entities.

As a 'constant' it enters into very important relationships between fundamental constants, yet it is still the subject of large measurement programmes. It is a key to a possible new definition of the kilogram, the unit of mass, but it is not yet known with sufficiently small uncertainty to easily make the transition from the old definition to the new one. An enormous amount of effort has been spent in the course of the past few centuries on the determination of the Avogadro constant and its improvement: its measurement uncertainty was reduced by a factor of 10 every 15 years over the last 150 years, see *e.g.* a historical overview in [1]. Since 1980, efforts have been made towards a redefinition of the mass unit using two approaches: one of the approaches is based on the so-called Watt balance [2]. The other is based on the silicon pathway using a large Si single crystal of natural isotopic composition [3, 4]. In the latter case, a combined effort was started around 1994 by several national metrology institutes: An *ad hoc* Working Group on the Avogadro Constant (AWGAC) was formed under the CCM. In 2002, that was turned into a formal WG of the CCM: WGAC. In 2003, the growing of highly enriched silicon 28 crystals became obviously feasible [5] and an international agreement was signed by the member institutes of the WGAC to finance the development and production of highly enriched ^{28}Si. This enables the growth of an almost perfect, almost

© 2010 WILEY-VCH Verlag GmbH & Co. KGaA, Weinheim

isotopically pure ^{28}Si single crystal, permitting a renewed attempt to redetermine N_A to a combined uncertainty of $10^{-8}\,N_A$. In the following, the enormous technical challenge of this project is described.

In each phase of the availability, the enrichment of the Si isotopes have been checked in collaboration with leading laboratories such as Joffe Institute RAS in St. Petersburg, the Itoh Research Group at Keio University in Japan, and the Thewalt Research Group at the Simon Fraser University in Canada to investigate in parallel which qualities in enrichment and purity are necessary 'on principle' for new applications in solid state spectroscopy, in fundamental research in semiconductor technology and quantum computing, or in the case of cooled SYS optics.

2 The need for enriched silicon for the Avogadro Project and other modern applications in research and technology The desired number of atoms in a kilogram can be obtained by counting all silicon atoms in a mole. A practically perfect single crystal is required in order to achieve the demanded high accuracy. The international consortium in its earlier research programme has chosen silicon as the material from which the crystal is made. Silicon crystals are widely available – in the case of natural isotopic composition – and are almost perfect in structure and purity.

The Avogadro constant N_A can be derived from

$$N_A = \frac{M_{\mathrm{mol}}}{m_{\mathrm{Si}}} = \frac{nM_{\mathrm{mol}}v}{V_0 m}, \tag{1}$$

with v, volume, and m, mass of a sample, M_{mol}, silicon molar mass, and V_0, volume of the unit cell (with n atoms). The defining quantities in the above equation are both accessible through direct measurement, not requiring any assumption about other fundamental constants. From Eq. (1) it can be deduced that the Avogadro constant relates to quantities on the atomic scale and the macroscopic scale: N_A is nothing other than the ratio of the molar volume V_m and the so called atomic volume V_a, or the ratio of molar mass to atomic mass. The atomic volume is defined as the ratio of the unit cell volume divided by the number of atoms involved. To acquire the value practically, the following quantities must be measured:

(i) the volume occupied by a single Si atom: the lattice spacing of an almost perfect, highly pure silicon crystal is to be derived. This includes the precise determinations of the content of impurity atoms and Si self-point defects including vacancies and self-interstitials,
(ii) the macroscopic density of the same crystal, and
(iii) the isotopic composition of the Si crystal, with the three stable isotopes ^{28}Si, ^{29}Si, ^{30}Si for calculating the molar mass of the sample.

The first two tasks have been attempted by several national laboratories: the National Institute of Standards and Technology (NIST) in the USA; the Physikalisch-Technische Bundesanstalt (PTB) in Braunschweig, Germany; the Istituto Nazionale di Ricerca Metrologia (INRIM) in Torino, Italy; the National Measurement Laboratory (NMI-A) of Australia and the National Metrology Institute of Japan (NMIJ) in Tsukuba; and during the starting phase of the project, the National Physical Laboratory (NPL) in Teddington, United Kingdom. The determination of the molar mass, the third point stated above, has been actively pursued at the Institute for Reference Materials and Measurements (IRMM) of the European Community in Geel, Belgium, and the PTB during the final phase of the project. The cooperation is coordinated under the auspices of the Bureau International des Poids et Mesures (BIPM).

The molar mass M(Si):

$$M(\mathrm{Si}) = \sum f\left({}^{i}\mathrm{Si}\right) M\left({}^{i}\mathrm{Si}\right) = \left[\sum M\left({}^{i}\mathrm{Si}\right) R_{i/28}\right] \Big/ \sum R_{i/28}, \tag{2}$$

is obtained from the measurement of the isotope abundance ratios $R_{i/28}$ of the three stable Si isotopes ^{28}Si, ^{29}Si and ^{30}Si which are then combined with the molar mass values $M\,(^{i}\mathrm{Si})$ of the individual isotopes, all available with an uncertainty $<10^{-8}$, for ^{28}Si with $<10^{-9}$, although it is sufficient to measure only two ratios $R_{29/28}$ and $R_{30/28}$ and to calculate the third ratio $R_{29/30}$. Nevertheless all three ratios are measured directly, since the combination of the single values via $(R_{29/28}/R_{30/28}/R_{29/30}) = 1$ can be used as a check. A deviation from 1 indicates systematic errors in the measurement of at least one isotope, which would show up in two amount ratios but not in the third one. To calibrate the measurement of $R_{i/28}$, IRMM used gravimetrically prepared synthetic mixtures from highly enriched ^{30}Si, ^{29}Si and ^{28}Si.

To achieve a further reduction in the uncertainty of N_A, an improvement in the molar mass determination is needed. This can be realised by fabricating an isotopically almost pure Si single crystal of $\geq$0.9999 enriched ^{28}Si, which means ^{29}Si and ^{30}Si abundances of the order of 0.00005 [6]. A relative combined uncertainty of $\leq$1% for each of these abundance-value corrections contributes a relative uncertainty to the molar mass value of the highly enriched ^{28}Si of $\leq 3 \times 10^{-8}$. Using this concept, the task is now to measure the (very) small ^{29}Si and ^{30}Si abundances in the highly enriched ^{28}Si again using synthetic isotope mixtures. That results in (very) small corrections to the molar mass value of ^{28}Si, known to a relative combined uncertainty of $\leq 10^{-9}$. Only the uncertainty of these small corrections will be included in the uncertainty budget of the molar mass of the highly enriched ^{28}Si in the Avogadro crystal. These corrections will be directly measured, but a critical point of these measurements could be the contamination of the enriched material by natural silicon, which is everywhere.

Besides the metrological application of enriched silicon material for a new definition of the mass unit kilogram, highly enriched isotopes with the atomic mass numbers 28, 29 and 30 refer to essential new materials for the fulfilment of

a series of international scientific projects and solutions to the following important scientific and technical problems:

Using ^{28}Si monocrystals with enrichment >0.9999 and a very low concentration of O, N, P, B and Al as developed in the Avogadro Project, a lot of on principle new results in research and technology have been shown in the field of

(i) Solid state spectroscopy in Si monocrystals
(ii) Spintronics in ^{28}Si crystals for new proposals in quantum computing
(iii) Thermal leakage by enhanced thermal conductivity of ^{28}Si compared to natural Si

Thewalt, Cardona and coworkers have shown [7–9] that smaller amounts of ^{29}Si and ^{30}Si atoms in a nearly perfect ^{28}Si crystal matrix are responsible for a reduction in the phonon–phonon interaction. It also causes the vanishing of fluctuations of the isotopic shift of the spectral lines, which makes thus far non-detectable transitions measurable quantitatively, *e.g.* the Zeemann hyperfine structures from the doublet of the ground state into the four states of the bound electrons of the excited state (see Fig. 17 in Section 6). It could be shown that new kinds of spectroscopic investigations at the energy levels of the Si crystal can be performed if the abundance f_{28} of the ^{28}Si atoms exceeds values of 0.99985 and the concentration c_O of the oxygen atoms is less than 10^{16} atoms/cm^3, provided a 'high-end' photoluminescence device is used.

The work of the Itoh et al. at the Keio University in Japan [10, 11] in the field of quantum computing based on ^{28}Si technology has opened new applications for Si isotopes: in the ^{28}Si matrix, structures of spin-carrying atoms are generated, such as ^{29}Si atoms or ^{31}P atoms, introduced by neutron transmutation reaction:

$$^{30}\mathrm{Si} + \mathrm{n} \rightarrow {}^{31}\mathrm{Si} \rightarrow^{\beta}\rightarrow {}^{31}\mathrm{P}. \qquad (3)$$

Devices based on the high-quality Avogadro material and prepared according to Eq. (3) show coherence times which are superior by many powers of magnitude to all known qubit devices for quantum computing. For further research in the field of 'All Si quantum computing' suitable Si material is now available, but it becomes also evident that the need for increasing the enrichment up to 0.999 995 and more is a future challenge.

Of possibly great importance is the application of ^{28}Si monocrystals for the leakage of high thermal load on optical devices such as monochromators or mirrors used in present or future generations of synchrotron sources and free electron lasers. These facilities consist of a large number of beam lines, each equipped with various optical components where the heat leakage can be enhanced by a factor of 30, if the Si mirrors normally operated at nitrogen temperature are exchanged by ^{28}Si mirrors cooled down to 20 K. Under these conditions, the optical system is more stable due to the extremely small thermal expansion coefficient α in this temperature region. For these applications, an enrichment of better than 0.999 seems to be sufficient and more economical than the highly enriched Avogadro material. The exchange of extremely expensive diamond windows in gyrotrons for ^{28}Si windows is currently under discussion at the IAPh RAS in Nizhniy Novgorod.

The application of enriched silicon in terahertz lasers and in SLS structures is under development. Important results have been published recently [12, 13]. It seems today that the quality of the Avogadro material fulfils the technical conditions also for these applications.

3 Initial attempt with ^{28}Si material (1994) An initial attempt was started in 1994 at PTB [5] when two sources of enriched material were available from the Oak Ridge National Laboratory (ORNL), USA, and from the National Institute of Metrology (NIM), Russia. The enrichment of both materials was similar: 0.9989 and 0.9988, respectively, see Table 1. Because the material delivered by the NMI in the form of 590 g of Si powder was found to be contaminated by an undesirably high amount of impurities, only the ORNL material – about 1284 g of $^{28}SiO_2$ grains – has been converted into a single silicon crystal in collaboration with the Wacker-Chemitronic company in Germany.

In order to avoid any loss of material or isotope enrichment, the following technical and chemical processes were applied:

(i) Reduction of SiO_2 to Si with high-purity aluminium powder at 1100 °C in a closed system: $3SiO_2 + 4Al \Rightarrow 3Si + 2Al_2O_3$.
(ii) Separation of the two end products using a chemical gas transport reaction in the presence of Te.
(iii) Growing a single crystal from the ^{28}Si melt in a quartz crucible [Czochralski (CZ) method], a method perfected by the Wacker company. A small natural Si crystal was used as a seed crystal. For further refinement, the material was melted and grown again, but instead of natural silicon, part of the CZ-^{28}Si crystal was now used as a seed crystal.
(iv) In the final step, floating-zone (FZ) crystal growth enabled reducing the amount of specific impurities, *e.g.* Al and P. For carbon and oxygen, a content of 1.3×10^{17} and 1.1×10^{16} cm^{-3} was determined by charge particle activation analysis. Unfortunately an unexpected residual content of about 10^{18} cm^{-3} boron atoms was found, the source of which was not recognised during the manufacturing process.

Table 1 Results of isotopic measurements by ion gas mass spectrometry at IRMM.

	^{28}Si	^{29}Si	^{30}Si	
$^{28}SiO_2$ (ORNL)	0.998875(16)	0.0799(14)	0.0326(12)	powder
^{28}Si (ORNL)	0.990176(10)	0.6025(4)	0.3799(10)	crystal
^{28}Si (NIM)	0.998805(30)	0.0872(24)	0.0323(18)	powder

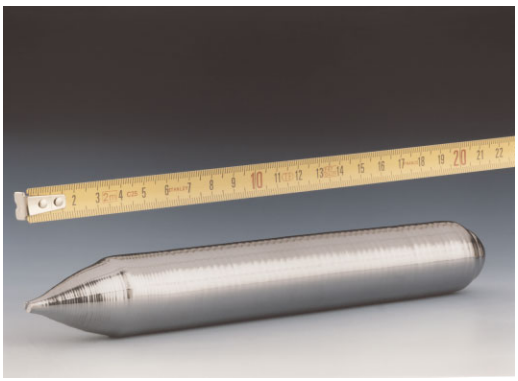

Figure 1 (online colour at: www.pss-a.com) The ^{28}Si crystal, about 215 mm long and 30 mm in diameter. The crystal is of ⟨111⟩ orientation.

The end product, the first ^{28}Si single crystal, had a mass of about 300 g and an enrichment of 0.9902, as shown in Fig. 1. The enrichment was unexpectedly diluted. The derived data for the Avogadro constant were about 10^{-5} larger than the data of previous measurements and not in agreement with the CODATA value published in 1986, possibly due to the insufficiently low perfection of the lattice and/or to an undetected contamination during the molar mass determination by natural silicon.

4 Second approach to perfect ^{28}Si crystals (1998–2000) In the 1990s, scientific interest and the technological promise of highly enriched isotopes led to a sharp rise in the number of experimental and theoretical studies with isotopically controlled semiconductor crystals. A contract for a feasibility study was signed between PTB, VITCON Projectconsult and former nuclear technologists in Russia, in St. Petersburg und Nizhniy Novgorod, to make highly enriched silicon in which the enrichment is more than 0.999 ^{28}Si and in which the concentration of the main impurities such as B, N, C, O, Al are some orders less than in the first attempt described in Section 2.

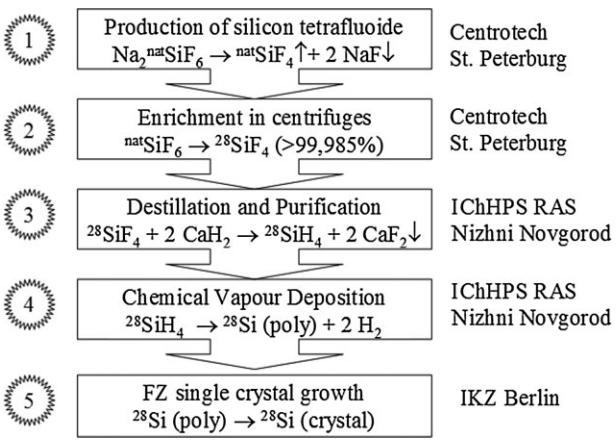

Figure 2 Production sites and main production steps of Si isotopes.

The collaboration of several institutes and their job sharing were the basis for all further developments, as shown in Fig. 2. High-purity silicon tetrafluoride gas has been used as the starting material for isotope separation and enrichment by means of the centrifugation method. On its basis, compact polycrystalline ^{28}Si was obtained. The entire process is discussed in more detail in Section 5.

Two charges (I and II) with various ^{28}Si content but having approximately the same chemical purity were prepared [14], for details see Table 2. No isotope dilution has been observed in any of the stages of conversion of silicon from tetrafluoride to solid crystal. The raw material in charge I was a grained polycrystalline silicon. On its basis, the feed rod, 20 mm in diameter and having a length of about 30 mm, was pulled from a quartz crucible by the CZ method to form a nonperfectly monocrystalline feed rod to continue the process with crucible-less FZ methods. The feed rod was subject to the zone refining process five times to reduce the impurity concentration. During the sixth run, a thin (2 mm) single crystal seed of natural silicon was used to finally start FZ single crystal growth in an Ar atmosphere. To minimise the isotope dilution and to eliminate dislocations, a Dash thin neck, 50 mm long, was grown. The left part of the crystal in Fig. 3 shows gliding dislocations originating from impurity segregation and precipitation, probably due to carbon. It is well known that an over-saturation of carbon in the molten zone typically causes twin boundaries followed by a polycrystalisation process.

The raw material of charge II was a compact polycrystalline feed rod with a diameter of 20 mm purified by the crucible-less FZ method. The growth process was similar to that of charge I but with a final run in vacuum. In Table 2, the isotopic composition of the crystals are summarised. Theses samples opened the door to first precise measurements of the thermal conductivity κ and for first precise estimates for the role which ^{28}Si crystals can play in microelectronic and epitaxial layer systems. Earlier misconceptions could be corrected.

5 Development of monoisotopic Si crystals (2000–2002) The feasibility study on the large-scale production of high-purity ^{28}Si in accordance with the Avogadro project was funded between 2000 and 2002 by the International Science and Technology Centre (ISTC), Moscow, and coordinated by VITCON – Project-consult in Jena. A first upgrade of the enriched amount of silicon-28 up to a dislocation-free single crystal with a total mass target of 300 g and an enrichment of more than 0.999 was

Table 2 Isotopic composition of polycrystalline samples, charge I measured at PTB by prompt n-γ-method, charge II measured by spark-mass-spectral method at IChHPS.

	^{28}Si	^{29}Si	^{30}Si	mass (g)
charge I	0.998588	0.1272	<0.2	11
charge II	0.99896	0.09	0.014	9

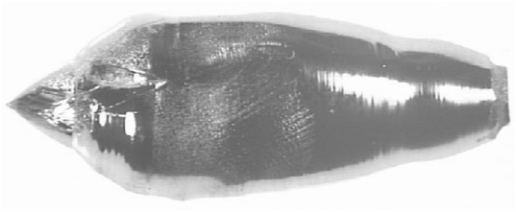

Figure 3 ^{28}Si crystal from charge I, right part is dislocation-free.

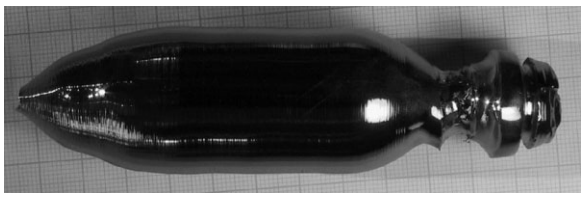

Figure 4 Final ^{28}Si crystal of the ISTC 1354 collaboration.

implemented within the framework of the ISTC project no. 1354. In seven production steps, the enrichment of ^{28}Si could be increased from 0.99896 to finally 0.9998, whereby for the last test (charge 7) an enrichment of 0.99995 for the SiF_4 gas could be demonstrated, see Table 3.

The end product of this project is shown in Fig. 4. The central part was dislocation-free and used for investigations connected to the Avogadro project. The impurity concentration was in the order of $8.2 \times 10^{14}\,cm^{-3}$ for oxygen and of $3.4 \times 10^{15}\,cm^{-3}$ for carbon. Positron annihilation [15] and laser scattering tomography [16] were applied to vacancy and void detection. Rather unexpectedly, a number of $10^5\,cm^{-3}$ voids could be found, but they were probably caused by the high amount of oxygen and hydrogen. The presence of voids indicated structural imperfections in the crystal lattice. An upper limit of less than $10^{14}\,cm^{-3}$ mono-vacancies was estimated by both methods. The density of the sample was also measured in comparison to the density of a natural isotopically composed silicon material.

The 'light' ^{28}Si isotopes are collected at one outlet of the centrifuge cascade, whereas the heavier fraction is separated by a lengthy process at the opposite outlet of the cascade, first in $^{30}SiF_4$ with an enrichment of 0.991. From the final fraction $^{29}SiF_4$ with 0.885 enrichment is produced. From these $^{29}SiF_4$ and $^{30}SiF_4$ 'by-products', also small ^{29}Si and ^{30}Si single crystals were grown with enrichments in the order of >0.99 [17], as shown in Fig. 5. They are used for the production of synthetic isotope mixtures to calibrate special ^{28}Si mass spectrometers for the Avogadro project and for fundamental research in the fields of solid state spectroscopy, spintronics, superlattice structures (SLSs), NDT production of ^{31}P from ^{30}Si, and so on.

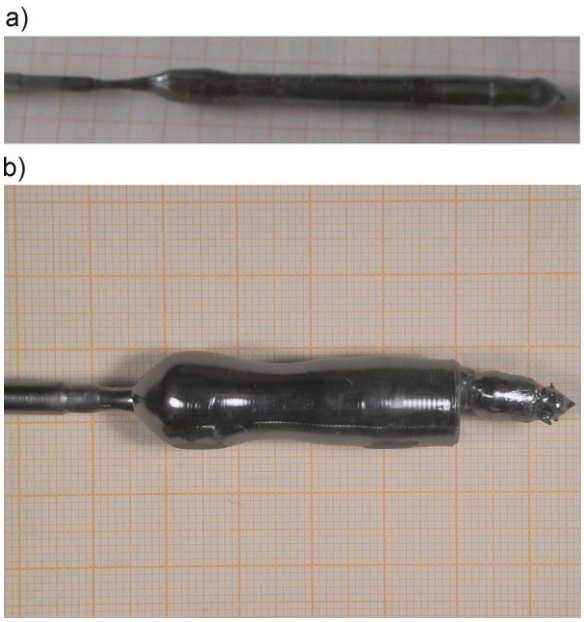

Figure 5 (online colour at: www.pss-a.com) ^{29}Si (top) and ^{30}Si single crystals with mass of 18 and 11 g, respectively.

6 Large-scale production of highly isotopically enriched ^{28}Si (2003–2006) From the output of the project no. 1354, a further reduction in the uncertainty of measured mean molar mass values (and hence of the value of N_A) by the fabrication of a 1 kg Si single crystal sphere of ≥ 0.9999 enriched ^{28}Si seems to be feasible. Two new ISTC projects (nos. 2630 and 2980) provided the financial frame, again with partners from Nizhniy Novgorod and St. Petersburg. The first project was financed – again – by the European Community as a member of the ISTC Foundation, the second by the metrology institutes themselves. The project task was the growth of a 5 kg single enriched crystal with the following boundary conditions: it must be isotopically homogeneous, which means that the isotopic contamination must be absent during the transformation of gaseous SiF_4 (the form in which the Si is enriched in the isotope ^{28}Si) in the several reduction steps to elemental Si (from which the single crystal is grown). Some contamination by natural

Table 3 Results of R&D in the framework of ISTC project 1354.

charge	1 + 2	3	4	5	6	7
^{28}Si	0.99896	0.9987	0.9993	0.9944	0.9994	0.9998
mass ingot (g)	20	50	46	32	46	190
mass crystal (g)	6	13	19	10.5	32	75
month/year	02/2000	04/2001	09/2001	11/2001	12/2001	06/2002

silicon from dust, quartz crucibles, *etc*., is acceptable if the contamination is homogeneously distributed throughout the material. The requirements for the chemical purity of this enriched ^{28}Si material are very stringent. However, isotope enrichment usually has the effect of a chemical purification process. So rather pure enriched isotope materials may be expected from the enrichment process. The costs of ~2 million Euro for 5 kg of a ^{28}Si monocrystal were shared by the European Commission, the national metrology institutes involved, the ISTC, and the partner institutes of the Russian Confederation.

The delivery of the enriched material to the participating metrology institutes was scheduled for 2006. A structured task distribution between the participating laboratories was implemented on a worldwide scale under the aegis of the Working Group on the Avogadro Constant of the Consultative Committee for Mass and Related Quantities of the CIPM. It coordinates the efforts undertaken by various national metrology institutes and research laboratories to determine this fundamental constant. The target uncertainties of the values are set for each of the quantities involved, which are to be achieved by each of the contributing institutes, such that an acceptably small relative uncertainty for the Avogadro constant approaching 10^{-8} can be reached [18].

The CIPM resolution no. 12/2007 has recognised the Avogadro project as an important initiative in the field of fundamental metrology. It considers the project to be an important new approach to international collaboration in metrology between national metrology institutes (NMIs), and between NMIs and other scientific institutes, on projects beyond the capabilities of an individual NMI or even an individual research laboratory. It has encouraged all NMIs to participate in and contribute to the project to the maximum extent possible, and it has encouraged NMIs participating in the project to develop an effective mechanism for formalising contributions, commitment and evaluation. The CIPM has invited the CCM to establish a special committee to oversee the implementation of effective mechanisms to coordinate the Avogadro collaboration and to keep the CIPM informed of the progress by providing an annual report and evaluation assessment: The International Avogadro Coordination (IAC) was launched in 2004 and has been working successfully since then.

The production of the highly enriched silicon isotope ^{28}Si begins with the transformation of Na_2SiF_6 powder to silicon tetrafluoride (SiF_4). The next and most crucial step is the ultracentrifugation of the gaseous (SiF_4) in sophisticated cascades of centrifuges in order to extract $^{28}SiF_4$ from the natural isotope mixture. Then, $^{28}SiF_4$ is chemically transformed to monosilane $^{28}SiH_4$ followed by cryogenic rectification of ^{28}Si, and then elementary ^{28}Si is obtained by pyrolytic deposition at ~850 °C on a ^{28}Si filament (slim rod) ~5–6 mm in diameter which was prepared beforehand. In this way, a cylindrical polycrystalline ^{28}Si rod is produced as starting material for the following FZ single crystal growth. The production of ^{28}Si single crystals is described in detail by the Technical Road Map (TRM28) [19]. Part 1 decribes the important operations, equipment and products necessary to grow an FZ single crystal which meets the goals of the Avogadro Project (TRM28OEP). Part 2 of the TRM deals with the analytical monitoring of the isotope enrichment, chemical purity and measurements of the crystal perfection, together with the way of certification (TRM28AMC). In part 3, the sample identification system (SIS) (TRM28SIS) is discussed, together with the code system for sample traceability through the whole technological chain of TRM28OEP and the distinctive assignment of the measurements according to TRM28AMC to the technological intermediate stages. In Table 4, a detailed flow charge of part 1 of the TRM is given.

6.1 Silicon tetrafluoride SiF_4 was used as the starting substance for the production of ^{28}Si. It was produced by the following chemical reaction from Na_2SiF_6 powder:

$$Na_2SiF_6 \rightarrow 2NaF \downarrow + SiF_4 \uparrow , \quad (4)$$

isotopes were separated by ultra-centrifugation (Fig. 6) [20].

Table 4 TRM28OEP: main stream of operations (Op) and products (Pr).

Op1: conversion of Si to Na_2SiF_6
Pr1: Na_2SiF_6
⇓
Op2: pyrolyse in ZT- reactor
Pr2: SiF_4
⇓
Op3: isotope enrichment in centrifuge- cascade in ZT
Pr3: $^{28}SiF_4$ – gas
⇓
Op4: conversion to isotop. silane
Pr4: $^{28}SiH_4$ – gas
⇓
Op5: purification of $^{28}SiH_4$ from fluor-containing impurities
Pr5: $^{28}SiH_4$:
⇓
Op6: rectification of isotop. silane
Pr6: i-purified silan
⇓
Op7: pyrolytic decomposition on Si slimrods
Pr7: polycrystalline ^{28}Si rods
Op8: homogenising and purification by CZ- growth from coated crucible and dross removing
Pr8: CZ-grown ingot for FZ-purification
Op9: purification by FZ crystallisation (crucible free)
Pr9A: purified ingot for final FZ single crystal growth
⇓
Op10: final crystallisation in defined direction and specified dimensions
Pr10: raw-crystal with defined specifications (crystal-orientation, dimensions)
⇓
Op11: cut of the crystal for sphere
Pr11: crystal for Avogadro sphere

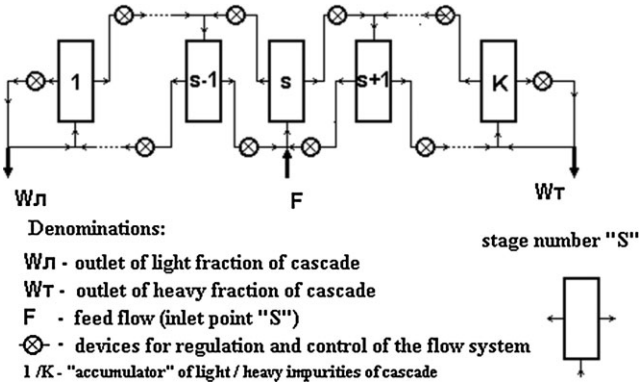

Figure 6 Scheme of the ultracentrifuges developed by CT in St. Petersburg, adapted to the Si- production. Acceleration 5×10^6 ms^2, 500 000 g.

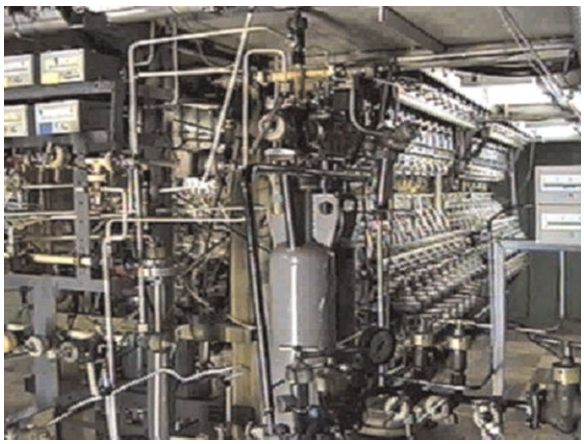

Figure 7 (online colour at: www.pss-a.com) The arrangement of 260 centrifuges for the $^{28}SiF_4$ production.

The elaboration of the technology to produce the high-purity, highly enriched ^{28}Si isotope by gas centrifuge cascades was carried out in two stages:

(i) First stage – the optimisation of the technology of enrichment of the ^{28}Si isotope and the modernisation of the separation unit to improve the chemical purity of $^{28}SiF_4$.
(ii) Second stage – the increase in separation power of the cascade on the basis of the scaling of the installation.

During the execution of the first stage, the significant differences between theoretical and practical values of isotope abundance of ^{28}Si in the product outlet of the cascade was determined. In particular, instead of the theoretical value, *i.e.* of ^{28}Si isotope 0.9999 the value of 0.9994 was received, in practice. It was caused by the silicon-containing impurities such as Si_2F_6O, SiF_3OH and others, which came into the cascade with the feed flow and appeared in a cascade during the process of isotope separation. The cascade units to separate the impurities from the product ($^{28}SiF_4$) were elaborated and applied [21]. As the result of this work, *e.g.* an enrichment 0.9999661(46) of ^{28}Si was achieved. In the second stage, the investigations in order to increase the accuracy of maintaining the mode of enrichment of the ^{28}Si isotope have been conducted. With the usage of special control systems, the long-time stability of maintaining, *i.e.* the ^{28}Si isotope at the cascade outlet was $\pm$0.001 l/d for more than 6 months.

Also in the second stage, the modernisation of a cascade was carried out with the aim to increase the productivity and efficiency of the separating process:

The number of gas centrifuges was doubled. The configuration of an 'ideal cascade' to separate multi-isotope gases was implemented. This configuration provides the exclusion of the mix of flows with different enrichments of ^{28}Si isotopes within the cascade. A new arrangement of 230 centrifuges in cascade was used to achieve a higher enrichment and productivity (see Figs. 7 and 8). The isotope enrichment measured of the final amount of $^{28}SiF_4$ (7294 g ^{28}Si) (average overall deliveries) is 0.999 928, as shown in Fig. 9.

6.2 Silane For the production of high-purity silicon the hydride method was used. As the first step, the synthesis of monosilane was carried out by the interaction of high-purity silicon tetrafluoride with calcium hydride:

$$^{28}SiF_4 + CaH_2 = {}^{28}SiH_4 + 2CaF_2. \quad (5)$$

The synthesis was carried out in the flow-through mode. The mixture of hydrogen with $^{28}SiF_4$ was passed through the reactor with fine-dispersed calcium hydride. The reactor was made of high-purity Si-free stainless steel to prevent the immission of natural Si and boron compounds into the highly enriched gas. The temperature of the synthesis was $\sim$180 °C.

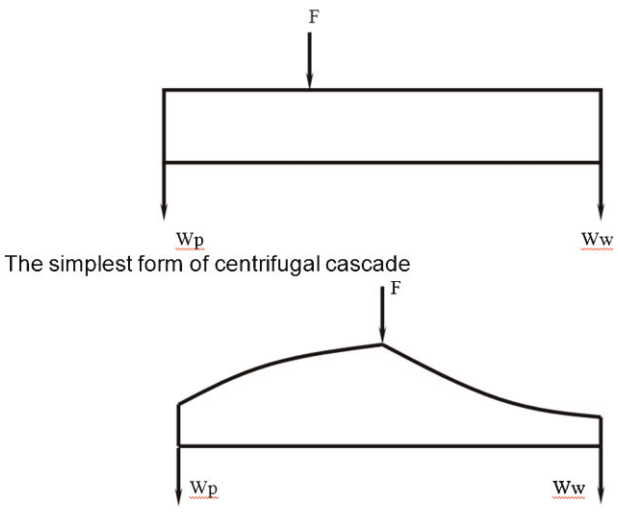

Figure 8 Optimised profile of the centrifuges for better productivity and enrichment.

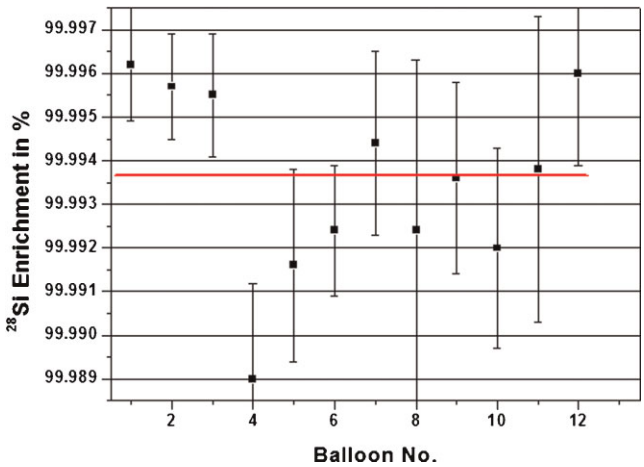

Figure 9 (online colour at: www.pss-a.com) Enrichment of $^{28}SiF_4$ gas over a production period of 6 months. Total amount of $^{28}SiF_4$: 27.71 kg (^{28}Si: 7.883 kg).

The conversion efficiency of silane exceeded 90%. The reaction was carried out without organic solvents to prevent silane contamination with carbon.

The content of hydrocarbons in silane measured by gas chromatography corresponds to their concentration in tetrafluoride.

Fluorine-containing compounds (fluorine containing siloxanes) and the light hydrocarbons C_1–C_4 are the main contaminants in the monosilane synthesised. For ultra-purification of silane, the methods of cryofiltration and rectification were consecutively used [22]. Cryofiltration carried out with low temperature (sub-cooled) boiling allows a preliminary purification of monosilane from the low-volatile impurities and from contaminations in the form of finely dispersed, suspended particles. For ultra-purification of silane from hydrocarbons, the method of rectification was used. This process was carried out in a stainless steel column with the feeding reservoir placed in the centre of the column in the periodic-mode operation. The fractions enriched with compounds having boiling points lower or higher than that of silane were removed simultaneously from the top and bottom parts of the column, respectively. The concentration of C_1–C_4 hydrocarbons in the selected fractions was monitored by gas chromatography. Residual hydrocarbons in the silane were reduced by more than a factor of 100 by ultra-purification.

6.3 Polycrystalline silicon Polycrystalline silicon was produced in a specially designed chemical (or better, pyrolytic) vapour deposition (CVD) set-up, characterised by a vertically placed cylindrical ^{28}Si rod. In this way, the whole deposited ^{28}Si could be processed later by the crucible-free FZ technique for further physical purification and single crystal growth. The $^{28}SiH_4$ silane deposition started on a ^{28}Si slim rod of 0.9999 enrichment, previously grown at the IKZ by means of the pedestal technique using a ^{28}Si from an older batch as feed rod; the slim rod diameter was 7 mm. It was aluminium-doped to about 0.5 Ωcm in order to facilitate the heating up with DC current. Due to the small distribution coefficient of 2×10^{-3}, Al could be easily removed later by the FZ refining method.

The slim rod fixed between molybdenum current contacts was resistively heated. One of the electrode contacts was axially movable to compensate for the thermal expansion of the rod. The operating temperature was 800 °C and was measured during the whole deposition process with an optical pyrometer in order to automatically control the heating power, to hold the rod surface temperature constant. The silane feed rate was chosen in such a way so as to provide a heterogeneous process of silicon deposition. Because the diameter of the polycrystalline Si rod increases during the process, the supply rate of silane was continuously increased to hold the deposition rate of polycrystalline silicon constant at 0.05 mm/h.

Several steps were necessary in order to produce slim rods for the growth and the CVD process. The polycrystal 'family' for the final crystal is shown in Figs. 10–12.

Using the technique described by the TRM, a first polycrystalline silicon rod with a diameter of 24 mm and mass of 440 g was successfully produced with a silane conversation efficiency of 95%. Fig. 10 shows the as-deposited poly-^{28}Si rod in vertical position in the CVD chamber.

Using this method, the poly-^{28}Si was deposited homogeneously in axial direction. The small differences between the charges (see Fig. 9) are reproduced in radial direction, but in the following technological step of zone floating, these differences are homogenised.

The polycrystal of Fig. 10 was used for the growth of the feed rods for the final Avogadro crystal, partly shown in Fig. 11. To that end, the polycrystal was FZ refined in several steps. A minimum of at least seven FZ runs in an argon and a vacuum atmosphere were necessary to reach the final specifications in chemical purity. Figure 12 shows the as-deposited 6 kg poly-^{28}Si rod with molybdenum contacts on both ends.

A still unsolved question was the possible separation of the isotopes by thermal diffusion due to the temperature gradient during the thermal deposition. In the case of the vertical alignment of the reactor, the heavier 29 and 30 isotopes are more concentrated at the bottom than at the top of the reactor. A model experiment was performed using a silane of natural isotopic composition for the CVD process. It could be demonstrated that in the case of 92% ^{28}Si, the enrichment along the crystal rod (80 cm) was 0.00000093. Regarding an enrichment of more than 0.99985, the isotopic inhomogeneity is negligible at a 10^{-10} level.

6.4 Single crystal growth Particularly the initial oxygen and carbon concentrations in the as-deposited polycrystalline ^{28}Si were still too high to reach the project goals. Therefore the material was, first of all, more purified at the IKZ by crucible-free FZ treatment, both in a vacuum and in an argon ambience. In vacuum, oxygen evaporates as

Figure 10 (online colour at: www.pss-a.com) Polycrystalline silicon rod Si28-9.1Pr7, deposited from SiH_4.

silicon monoxide. Carbon is reduced by the segregation effect of multiple FZ passing. Due to the absence of sources of contamination with natural silicon, the isotope enrichment was not affected, assuming that ^{28}Si seed crystals were used. Finally, the C and O concentrations were pushed below the FTIR detection limits – at least at the seed-end of the FZ rod.

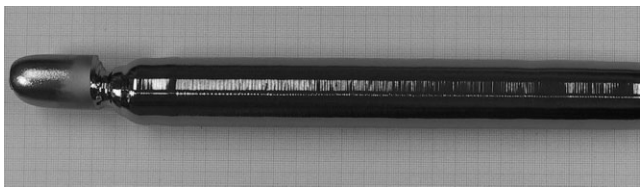

Figure 11 Crystal Si28-9.1Pr10, FZ-grown from the polycrystalline rod Si28-9.1Pr7, after one FZ run.

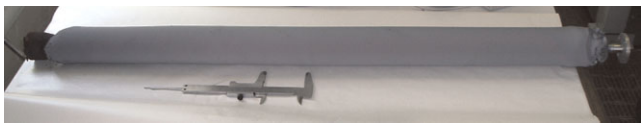

Figure 12 (online colour at: www.pss-a.com) The 6 kg polycrystal rod 28Si-10Pr7.

For the single crystal growth, a ⟨100⟩ oriented ^{28}Si seed of 0.9999 isotopic enrichment was previously grown by the crucible-free pedestal method.

In practice, FZ purification and subsequent ^{28}Si FZ single crystal growth were rather risky, see the course of development in Fig. 13. The first FZ run had to be interrupted because at the melting front, non-removable silicon spikes were formed. As a result, the polyrod (Fig. 12) was fragmented and a procedure to rejoin it by FZ had to be created. Also the socket part was broken during the third FZ run. It was decided to pull a little CZ crystal from the fragments and join it in the fourth FZ run, together with the tail-end of the main part. In the nineth FZ run, the diameter was increased to 85 mm to enable the growth of the final shape as shown in Fig. 14. The FZ runs were first carried out in vacuum and later in an argon atmosphere where the low oxygen concentration was saved by a previous long-time desorption of the water layers in vacuum.

After FZ purification, only ∼4.8 kg ^{28}Si remained for the growth of the final crystal. Therefore, it had to be grown with varying diameters in order to enable the preparation of two 1 kg spheres, together with a number of auxiliary samples for material characterisation. This was successfully achieved by programming the automatic diameter control system. At the end of the growth process the crystal was grown tapered down to a diameter of 60 mm. The final crystal was of p-type with a mass of 4530 g. Only a small end part of about 200 g was disturbed by back-gliding dislocations. Most of the impurities are accumulated in the other residual parts – with a total mass of ∼1 kg – but the ^{28}Si isotopic enrichment was not affected. This material is still available for other research needs in addition to the Avogadro project.

6.5 Crystal characterisation The results of the analysis of the isotopic composition as well as of the oxygen and carbon contents of the ^{28}Si single crystal are shown in Table 5. The samples for the analysis were cut from different parts of the crystal according to the cutting diagram of the IAC shown in Fig. 15. An isotopic analysis was made by laser mass spectrometry (LIMS) at the IChHPS RAS and by electron impact gas mass spectrometry (EIGSM) at IRMM and by special SIMS measurement at IPhMS RAS in Nishny Novgorod. The results show that the content of the ^{28}Si isotopes in the crystal exceeds 0.999 94. The oxygen and carbon concentration in the ^{28}Si single crystal was measured by IR spectroscopy (IChHPS RAS and PTB) and the method of laser ionisation-flight time tandem mass reflection of IhpS.

Figure 13 (online colour at: www.pss-a.com) Evolution of the ^{28}Si Avogadro crystal: the 28Si-10Pr7 poly rod (a) made by ICHPS in N. Novgorod from $^{28}SiF_4$ which was more than 0.9999 enriched by Centrotech/St. Petersburg was fragmented when the first FZ run had to be interrupted, but joined again by FZ (b: Pr10.1). When the socket-part in the third FZ run (c) got broken, a little CZ crystal (d: Pr10.Cz) was pulled from the fragments and joined in run 4 (e: Pr.10.4). In the nineth run, the diameter was increased to 85 mm (f: Pr.10.5) to enable the growth (run 9) of the final shaped crystal (g: Si28-10Pr11, Fig. 14).

The results indicate that this material is – so far – the purest ^{28}Si crystal ever grown with respect to electroactive impurities.

7 Applications of ^{28}Si crystal material and of ^{29}Si and ^{30}Si Besides the metrological application of enriched 28Si material for a new definition of the mass unit kilogram, highly enriched silicon isotopes with the atomic mass numbers 28, 29 and 30 refer to essentially new materials necessary for the fulfilment of a series of international scientific projects and the solutions to the following important scientific and technical problems:

(i) Solid state spectroscopy
(ii) Spintronics and quantum computers
(iii) Cooling of SYS-optics
(iv) Microelectronics
(v) SLSs and terahertz lasers
(vi) One-step deposition of Si from SiH_4 by PECVD

Figure 14 (online colour at: www.pss-a.com) Final FZ crystal with code number Si28-10Pr11.

7.1 Determination of the Avogadro constant A detailed description of the measurement procedures to be applied to the silicon material and a value for the Avogadro constant with a relative measurement uncertainty close to 1×10^{-8}, to be derived from those results is given in [23]. At present, the participating institutes are improving their measurement capabilities with samples from the naturally composed sample WASO04. A brief status of the present uncertainty reached is summarised in the following:

According to Eq. (1), containing the quantities to be measured, the individual steps of the density determination of the ^{28}Si silicon spheres were:

(i) Diameter measurements of sphere in vacuum at 20 °C using an optical Fizeau interferometer [24]. A measurement uncertainty of 0.3 nm in the diameter determination has been reached. This result approaches the project target.
(ii) Mass and density measurements of the oxide layer for optical phase shift and mass correction. Because of the insufficient knowledge of the stoichiometry of the

Table 5 Impurity content and enrichment of ^{28}Si material.

charge	isotope	enrichment			
		in SiF_4	in SiH_4	in poly-Si	in Si-crystal
10	^{28}Si			0.99994543(82)	0.99994935(22)[b]
	C			$4.2^{a} \times 10^{15}\,cm^{-3}$	$0.34(40) \times 10^{15}\,cm^{-3}$
	O			$6.8^{a} \times 10^{15}\,cm^{-3}$	$0.21(1) \times 10^{15}\,cm^{-3}$
9.1	^{28}Si	0.9999661(46)[c]	0.999 930(17)[d]	0.999905(22)[d]	0.999909684(59)[c]
2	^{29}Si	0.99576(105)[d]		0.994 87(45)[d]	0.99239(23)[d]
2	^{30}Si	0.99829(60)[d]		0.997347(525)[d]	0.99722(22)[d]

[a]Result is calibrated and corrected for contamination. Oxygen and carbon concentration in the ^{28}Si crystal were determined by the method of IR-spectroscopy at PTB and the method of laser ionisation time-of-flight tandem mass reflection of IhpS; [b]results not calibrated and affected by contamination with natural isotopic composition, only; [c]and by electron impact GAS mass spectrometry (EIGSM) at IRMM; [d]isotopic analysis of the grown single crystal was made by LIMS at the IChHPS RAS.

polished generated oxide layer, the spheres are etched and covered with a thermal oxide. The mass of the oxide layer is determined by the measurement of the density of the oxide layer and its thickness. The oxide thickness varies since the growth rate of SiO_2 depends strongly on the crystallographic orientation. Therefore, a mapping of the oxide layer thickness on the sphere is required, which can be performed by spectroscopic ellipsometry. The absolute value has to be calibrated by X-ray reflectometry, XRR. The density of oxide layers can be directly measured by application of the so-called pressure-of-flotation method by stepwise thermal oxidation. A measurement uncertainty of 0.1 nm in the thickness determination has nearly been reached. A

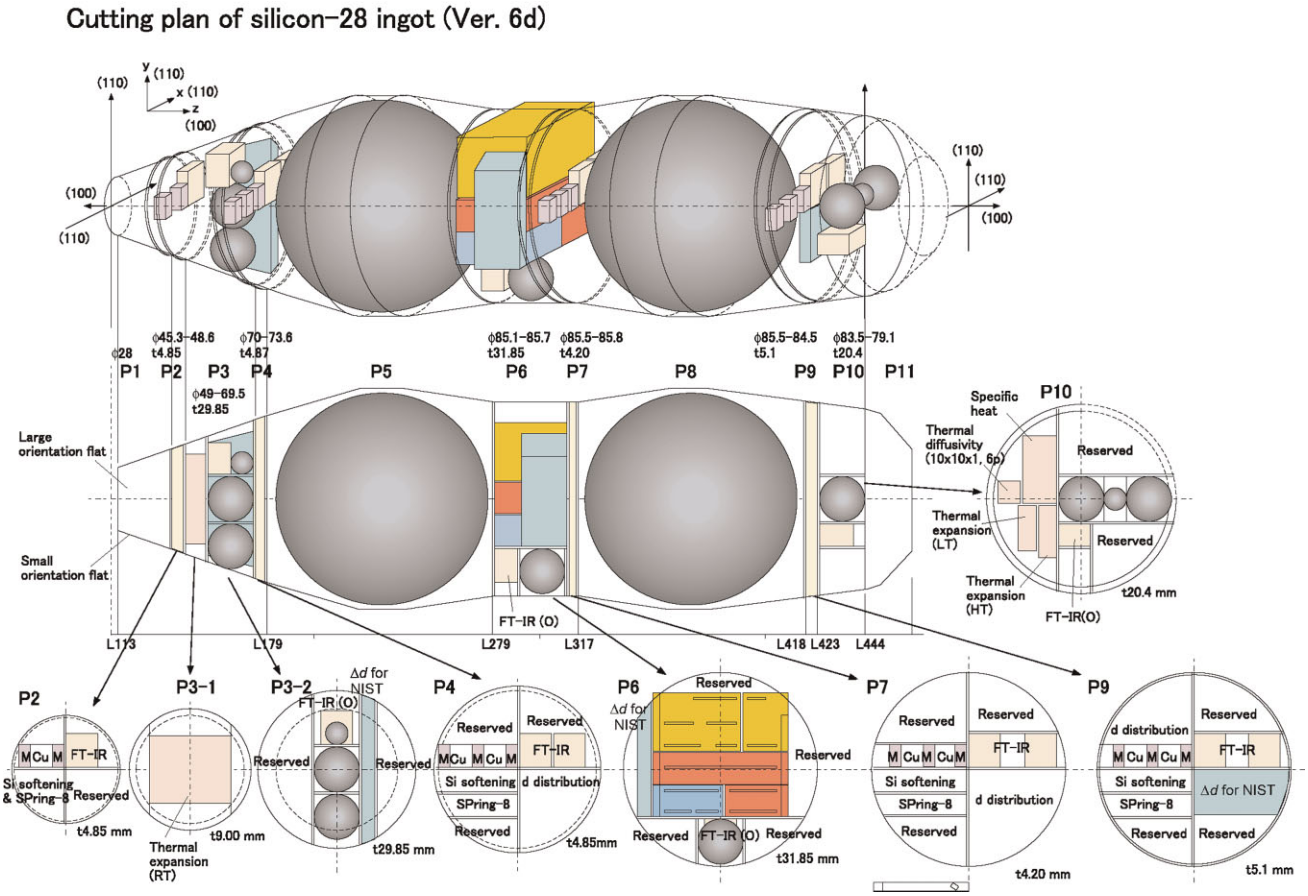

Figure 15 (online colour at: www.pss-a.com) Cutting schema for the two spheres and the 55 samples for measuring all relevant parameters of the final Avogadro crystal. (see Section 6.1).

measurement uncertainty of 0.5% for the density measurement has been reported. These results approach the project target.

(iii) The lattice parameter, a_0, of the ^{28}Si crystal is measured with a combined X-ray and optical interferometer capable of displacements of up to 5 cm. The measurement of the travelled distance with the optical interferometer and the simultaneous counting of the X-ray fringes provide the average lattice parameter over the examined crystal volume. This measurement is independent of the X-ray wavelength and is traceable to the metre via the frequency of the stabilised laser source. Assuming that the unit cell is cubic and that it accommodates eight atoms, the atomic volume is given by $V_o = a_0^3/8$. The new apparatus has been tested by integrating a new long interferometer manufactured from the WASO04 crystal to fully exploit the extended displacement capability. Preliminary measurements indicate a resolution and repeatability in a range of $5 \times 10^{-9} a_0$, which meets the project requirements.

(iv) Mass measurements of the spheres are performed in vacuum. Due to the different densities of mass standards and silicon, transfer standards for mass comparison with the prototypes in air are used. An estimate of the water layer on the sphere in air and vacuum was made. On the sphere, no hydrocarbon layer could be detected after cleaning. A measurement uncertainty of 5 μg in the mass determination has been reached. This result fits the project target.

(v) The molar mass is obtained from measurements of isotope abundance ratios of ^{28}Si, ^{29}Si and ^{30}Si. In the case of natural silicon, a relative measurement uncertainty of the order of 1×10^{-7} was achieved. A further reduction of the uncertainty can be obtained only by using the highly enriched silicon crystal. The molar mass determination is carried out at IRMM. Measurements on samples cut from the enriched ^{28}Si crystal are in progress, indicating a relative measurement uncertainty in a range of 1×10^{-8}, which fulfils the project requirements.

Preliminary measurements on enriched samples indicate for the Avogadro constant a relative resolution and repeatability of $\sim 5 \times 10^{-8}$. A systematic error in previous measurements in the order of 1 ppm is discovered and will be evaluated.

7.2 Solid state spectroscopy Recent investigations by Thewalt and coworkers using highly enriched silicon samples have demonstrated for the first time very promising results regarding the dependence of the phonon spectra on the isotopic mass spectra and isotopic disorder, which affect the electronic properties of solids by the mechanism of electron–phonon interaction, in particular by the corresponding optical excitation spectra and energy gaps [25].

In Fig. 16, the P bound exciton photoluminescence emission (PLE) line shape as a function of temperature T and enrichment E can be seen excited by a tuneable single-frequency Yb fibre laser ($\Delta h\nu = 0.3$ neV). From enrichments higher than 0.99985 all the overlapped and isotopic broaden lines are fully separated and so new and so far not yet feasible applications in solid state spectroscopy should be possible.

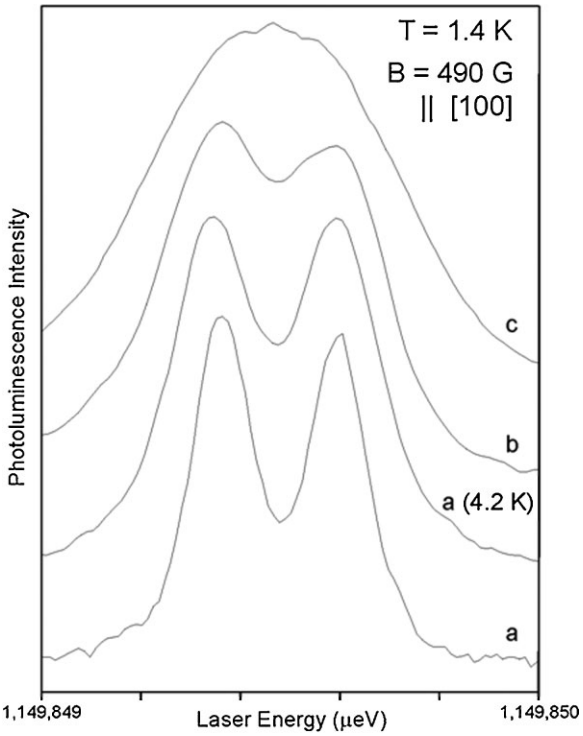

Figure 16 P-bound electron PLE line shape as a function of enrichment and temperature; (a) enrichment 0.99991 measured at 1.4 K (SIS-code Si28-9.1Pr11); a (4.2 K) the same at 4.2 K; (b) Si28-7Pr10 0.99983, 1.4 K; (c) Si28-halPr10: 0.9992, 1.4 K.

In Fig. 17, the hyperfine structure (Zeeman spectrum) of the phosphorous bound exciton (PBE) without phonon transitions in 0.99991 ^{28}Si is presented, measured by PLE and excited by tuned laser with an overall resolution of 0.3 neV. [8]

In this way, small concentrations of ^{31}P in highly enriched ^{28}Si crystals could be observed by either photoluminescence or photocurrent spectroscopy [26]. Bound excitons in boron could also be detected by these methods. With IR absorption measurements, neutral P donor and B acceptor levels in ^{28}Si, ^{29}Si und ^{30}Si could be measured. It could be also shown that the excited levels were one order of magnitude sharper than those observed in natural silicon [27]. Levels of sulphur [28] and selenium [29] atoms in ^{28}Si were also measured, which opens the way for new qubit constructions for quantum computer. One of the most promising constructions of qubits are ^{31}P atoms as neutral donors for bound excitons in >0.9999 ^{28}Si monocrystal pumped by tuned laser at 1149.850 meV, at 1.4 K and 435 G. The magnetic field is orientated parallel to the ⟨001⟩ direction of the Si crystal.

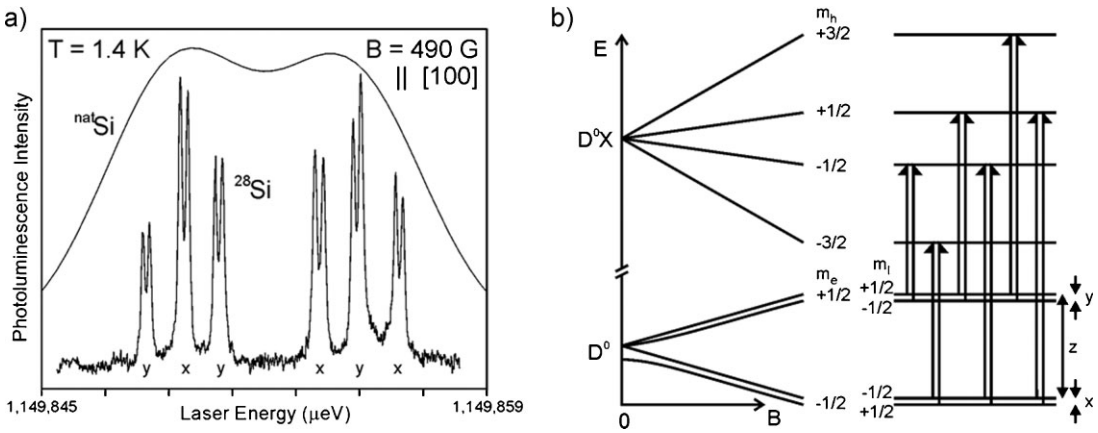

Figure 17 Hyperfine structure (Zeeman spectrum) of P BE no-phonon transitions in 0.99991 ^{28}Si measured by PLE, excited with tuned Laser 0.3 neV; application: detection of ^{31}P-dots in ^{28}Si- matrix (see also Section 6.3).

Figure 18 shows the neutral donor bound exciton transition and its Zeeman splitting in silicon [30]. In Fig. 18a, the two electrons (●) of the excited state D^0X are indistinguishable, forming a spin singlet which cannot couple to the hole (○), the nuclear spin, or the magnetic field. The Zeeman splitting of the ground state D^0 and the excited D^0X states, and the allowed optical transitions ordered numerically from 1 to 12 due to their increasing energy are shown in Fig. 18b. The hyperfine splitting of D^0 results in two parallel states, shown in black and two anti-parallel states, shown in red. The optical polarisation mechanism is schematically outlined in Fig. 18c. A single frequency laser pumps neutral donors (D^0) from only one selected electronic and nuclear spin state into an excited D^0X state. This state decays with high probability into an ionised donor plus a free electron accompanied by the predominant Auger decay of D^0X in silicon; subsequent electron capture may then populate the opposite electronic spin state. The pure nuclear relaxation rate is assumed to be negligible, and the pump rate is assumed to be much higher than either the optically enhanced electronic relaxation rate W, or the cross relaxation rate R. As a measured result, the photoconductivity spectrum of the ^{31}P bound exciton in the most perfect sample of ^{28}Si available is shown in Fig. 18d.

7.3 Application of Si isotopes in a quantum computer Based on the availability of highly enriched ^{28}Si crystals with $<5 \times 10^{-5}$ spin-carrying ^{29}Si isotopes, on the one hand, and relatively highly enriched ^{29}Si crystals with ½ nuclear spin, on the other hand Kohei and Itoh have proposed a quantum computer based on the well-known Si technology [31] and realised important elements of the

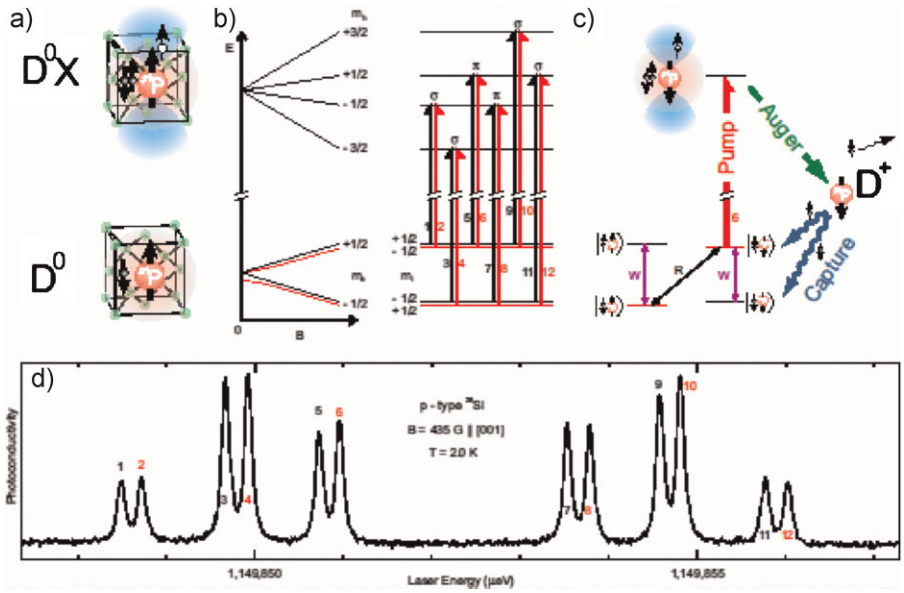

Figure 18 (online colour at: www.pss-a.com) The neutral donor bound exciton transition and its Zeeman splitting in silicon. (a) A schematic of the transitions between the neutral donor ground state (D^0) and the bound exciton ground state (D^0X). (b) Shows the Zeeman splitting. (c) Schematic for the optical polarisation mechanism. (d) A photoconductivity spectrum of the ^{31}P bound exciton in the most perfect available sample of ^{28}Si.

Table 6 Measurements of different electrical parameters of various Q-bit systems.

	qubit	$\omega/2\pi$	T_2	Q	ΩT_2	JT_2
atomic	trapped optical ions ($^{40}Ca^+$)	412 THz	1 ms	10^{12}	10^2	10^1–10^3
	trapped microwave ions ($^9Be^+$)	1.25 GHz	1 ms	10^6		10^1–10^3
	molecular nuclei in liquid solution	500 MHz	2 s	10^9	10^3	10^2
solid state	charge states in quantum dots	200–600 THz	40–630 ps	10^5	10^5	10^2
	Josephson-junctions flux qubits	6.6 GHz	30 ns	10^3	10^2	10^1
	Josephson-junctions charge qubits	16 GHz	500 ns	10^4	10^2	10^4
	Josephson-junctions phase qubits	16 GHz	5 μs	10^5	10^2	10^4
	^{29}Si nuclei in solid silicon	60 MHz	25 s	10^9	10^6	10^4

quantum computer technology as quantum dots and quantum wires. It is known that an important problem to be solved for the realisation of quantum qubits as carrier of the information is the achievement of a very long coherence time and other complex criteria, which were investigated by Ladd et al. [32, 33]. A result of their studies is that ^{29}Si qubits show, at room temperature, better data by four orders of magnitude than other solid state qubits such as Josephson elements, see Table 6.

The coherence time T_2 of various qubits was measured either by spin echo spectroscopy or by four-wave mixing; exceptions were noted. Q is the product of the fundamental qubit frequency $\omega_0/2\pi$ and πT_2. The ωT_3 column shows the experimental product of the Rabi frequency and the coherence time, thus providing a more realistic measure than Q for the sequentially available single gates. Technical improvements can increase ΩT_2 as far as Q in some architectures, whereas for others Q must be limited in order to maintain selective qubit control. The JT_2 column shows the product of coherence time and the measured or expected qubit-qubit coupling speed, roughly the available number of sequential two-qubit gates.

Another approach to the optical manipulation of spin qubits has been proposed by Thewalt et al. under the condition of a highly enriched high-purity ^{28}Si crystal matrix: in this case ^{31}P atoms can be detected by optical means. These ^{31}P dots can be formed by ^{30}Si neutron transmutation to ^{31}P using the well-developed Si semiconductor technology. (see also Section 6.5).

7.4 Cooling of synchrotron optics Synchrotron sources need optical elements in order to select monochromatic light and to deflect unwanted radiation from the spectra. For this task Bragg optics is usually used based on the X-ray diffraction by crystals. At the so-called 'last generation' of synchrotron sources, *e.g.* DESY in Germany, ESRF in France, and Spring-8 in Japan, the photon intensity is so high that the monochromator crystals are heated up, which results in a lattice deformation and thus in a reduced quality of the optical imaging. To overcome this difficulty, the silicon Bragg crystals are usually cooled down with liquid air, taking into account two features of the silicon crystals: The temperature conductivity increases with lower temperature, and at 120 K the heat expansion coefficient has a minimum value. But, new findings on the thermal features of enriched isotopes are not considered until now:

^{28}Si crystal material has, compared to naturally composed Si a higher thermal conductivity κ (see Fig. 19) and is higher than ever measured on dielectric material (higher than κ of diamond). This advantage is also valid for the thermal diffusion $D = \kappa/(\rho C_W)$ which is responsible for the heat transportation [34, 35] (see Fig. 20). Also, the lattice

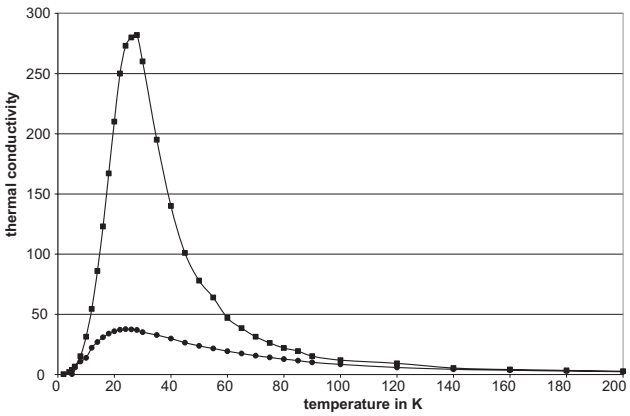

Figure 19 Thermal conductivity of natural (solid circles) and 0.9995 enriched ^{28}Si crystals (solid squares).

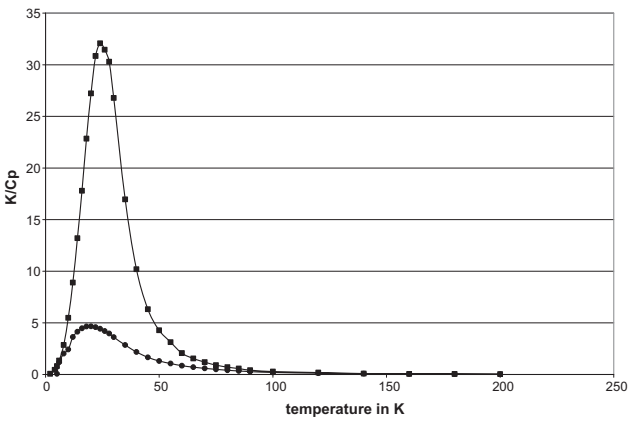

Figure 20 Thermal diffusion of natural (solid circles) and 0.9995 enriched ^{28}Si crystals (solid squares). Thermal diffusion is a measure for thermal transport in a thermal field. $D = \kappa/(\rho C_p)$, with κ thermal conductivity, ρ density, C_p thermal capacity.

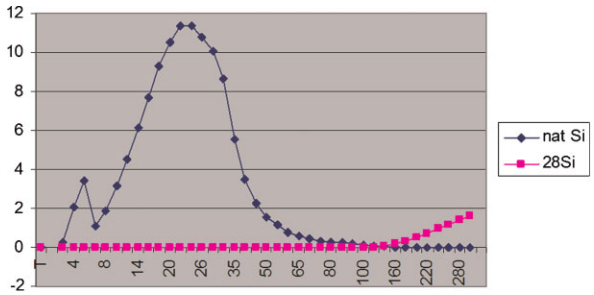

Figure 21 (online colour at: www.pss-a.com) Thermal lattice deformation $\delta \sim \alpha/\kappa$ of ^{28}Si and natural Si.

deformation $\delta \sim \alpha/\kappa$ due to heat load is significantly reduced (α linear thermal expansion coefficient), as shown in Fig. 21. Using ^{28}Si at 20 K temperature instead of naturally composed Si at the so-called low nitrogen temperature LNT, the following improvements can be expected:

(i) thermal deformation by a factor $>10^5$
(ii) heat transportation by a factor 4.

7.5 Application of Si isotopes in microelectronics At present, the electronic circuits of most semiconductor devices use *p–n* junctions made by implantation of the doping ions in a silicon substrate. Thus, the profile of a dopant is characterised by essential spatial fluctuations. These effects impair the performance of the semiconductor devices. For their perfection, it is necessary to decrease the lateral dimensions of the components, which requires a decrease in the depth of *p–n* junction, a decrease in the spatial fluctuation of dopant concentrations, and also an increase in the dopant concentration up to a level superior to solubility in a solid phase. The structure with these parameters can be obtained by neutron doping of the silicon isotope heterostructures. Neutron transmutation doping (NTD) occurs due to the ^{30}Si isotope n-transmutation to ^{31}Si, which, in turn, is unstable, with a half-life period of 2.6 ns, and transmutes into a ^{31}P isotope. Phosphorus is a donor dopant in silicon, and thus the NTD reaction results in generating *n*-type Si having a highly uniform dopant distribution. It is possible to produce the *p–n* junction with an smaller depth and atomically smooth boundary between *p* and *n* layers, growing an epitaxial layer with a predetermined thickness of ^{30}Si on a buffer layer, which may be p-doped ^{28}Si [36]. A concentration of 5×10^{16} to 6×10^{17} ^{31}P atoms/cm^3 in a 0.9 ^{30}Si MBE layer with an n dose of 7×10^{20} thermal neutrons/cm^2 were produced [37]. Of course, destructions of the Si lattice from the reaction $^{30}\mathrm{Si} + n \rightarrow {}^{31}\mathrm{Si} \rightarrow {}^{31}\mathrm{P} + \beta$ and from the small part of fast neutrons out of the reactor have to be taken into account. These effects were healed up after a 1 h annihilation at 700–800 °C.

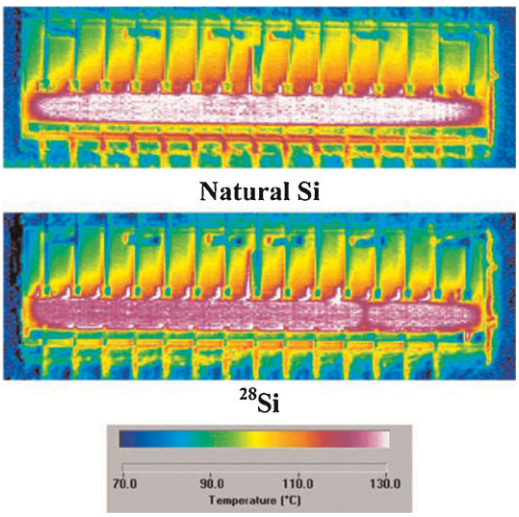

Figure 22 (online colour at: www.pss-a.com) Transistor package produced with 0.999 ^{28}Si, reduction of heat load by 5 to 7 °C at RT.

An important property of monoisotopic silicon differing from natural silicon is the above-mentioned higher thermal conductivity. This effect can be used in different electronic devices. For example, by the IR microscopy technique a clear reduction between 5 and 7 °C in the transistor average temperature and a corresponding 5–10% decrease in the overall package thermal resistance could be observed in devices fabricated using a ^{28}Si layer on top of natural silicon substrates, see Fig. 22 [38].

7.6 Superlattice structures (SLS) designed from Si isotopes From the first experiments of Osten and coworkers [39] determining the width of transitions in Si of different isotopic composition it could be deduced that transition widths of only a few nm could be possible. In [40], Itoh and coworkers demonstrated an amazing application: from ^{28}Si and ^{30}Si, they formed SLS structures of more than ten periods with 2.7 nm thickness and used them as a controlled scale of depth for the controlled implementation of as ions in Si crystals. Figure 23 shows an implanted 'hidden' as layer at a depth of 40 nm. This method can be used as a diagnostic tool for the design of structures in microelectronics if increasingly smaller dimensions are required.

In the future, the preparation of SLS from Si enriched isotopes will open the door for important developments and interesting solutions in semiconductor physics.

7.7 Is an enrichment >0.999 99 ^{28}Si possible? The principal objective of a new ISTC Project no. 3736 which is fully financed by the European Community with ~US$ 500 000 is the development of a technology for the direct production of high-purity and highly enriched silicon in the form of films and bulk polycrystals directly from the $^{28}SiF_4$- gas by non-equilibrium discharge of a mixture of silicon tetrafluoride and hydrogen using the

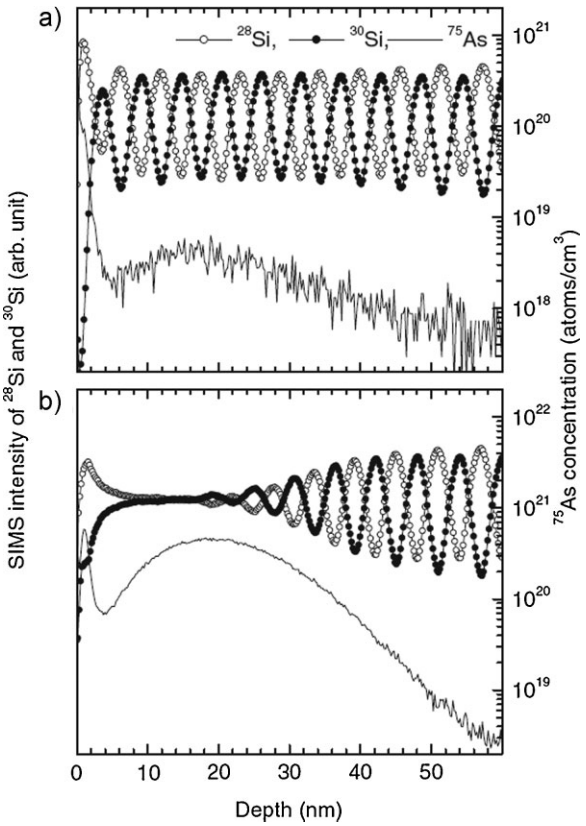

Figure 23 SLS of ^{28}Si/^{29}Si. Depth of period 2.9 nm, modified by As-implantation: depth profiles of ^{28}Si (open circles), ^{30}Si (filled circles), and ^{75}As (solid curve) measured by SIMS in the ^{28}Si(2.7 nm)/^{30}Si(2.7 nm) isotope superlattices after ^{75}As implantation at the energy of 25 keV with doses of (a) 1×10^{13} cm^2 and (b) 1×10^{15} cm^2.

plasma-enhanced chemical vapour deposition (PECVD) method. The target of the project is to develop finally ^{28}Si solid material, at a rate of several grams with given parameters of isotopic and chemical purity (silicon-28 – 0.99999, silicon-29 – 0.9997 and silicon-30 – 0.9997 enrichment), and a maximum yield (85–90%). The result of the project will be recommendations for the promising large-scale production of silicon isotopes and isotopes of other elements as highly enriched fluoride precursors (germanium, sulphur, selenium, *etc*.). The research will be done on the basis of the experiences of the IAPh RAS in plasma techniques and of the IPhM RAS (both in Nizhniy Novgorod) on micro- and nanostructural developments). The first charge of $^{28}SiF_4$- gas was produced by Centrotech St. Petersburg and measured by the IRMM to be 0.999 996 94 [41]. The first crystal of natural silicon directly produced from SiF_4- gas has been produced recently [42].

8 Conclusions At present, the metrology institutes involved are engaged in reducing the relative measurement uncertainty for the Avogadro constant from the 10^{-7} to the 10^{-8} level. Using single crystals of natural silicon, the uncertainty attained for that value, especially for the molar mass, has now reached practical limits. A further reduction of the uncertainty using a ^{28}Si crystal with 0.99995 enrichment has been internationally coordinated since 2003: within a cooperation of eight national institutes, international research institutes and two Russian R&D institutes, about 6 kg of highly enriched ^{28}Si material in the form of a polycrystalline rod have been produced and delivered to the IAC at the end of 2006. The FZ run for growing a single ^{28}Si crystal was successfully finished at the IKZ in May 2008, and two almost perfect 1 kg spheres were shaped and polished by the Australian National Research Cooperation CSIRO and handed over in April 2008 to the IAC. An initial inspection of samples showed that the isotopic and chemical composition of the material has met the requirements of the IAC.

In any future redefinition of the SI unit kilogram, there are good reasons for fixing a number as the ratio between the kilogram and the mass of an atomic particle, such as the mass of a carbon-12 atom. Compared with other proposals, such as fixing a numerical value of the Planck constant or of the frequency being equivalent to a kilogram, a link to a mass at the atomic level is more obvious and intrinsic to the unit of mass. To reach this goal successfully at the end of 2009, the work on N_A in the partner laboratories must be based on continuous interaction between physics and technology at their highest levels, and it would contribute to strengthening the edifice of the fundamental physical constants.

So far, a first inspection of the material has been started and the following characteristics of the material have been checked: impurity, vacancy and void contents, isotope enrichment and homogeneity, lattice parameter and density differences, presently compared with silicon of natural composition. All measured data so far fulfil the expectations of the scientists. For example, the carbon and oxygen content in the Avogadro crystal – regularly the dominant impurities in commercially available FZ crystals – is astonishing small.

The highly enriched and chemical pure crystal material produced by the international Avogadro consortium is the basis for further new research in solid state physics, for new technological solutions in semiconductor electronics and quantum computing and for new developments of high thermal load Bragg reflectors for synchrotron optics.

The Avogadro constant is not the only candidate in the running for a redefinition of the unit of mass. The so-called watt balance experiments which are being set up at several metrology institutes, such as, *e.g*. in the USA, England and Switzerland, are given better odds in expert circles of winning the competition. But matters have not progressed thus so far yet.

Acknowledgements We would like to thank our partners at the CENTROTEKH in St. Petersburg (A. K. Kaliteevski and O. N. Godisov) and at the Institute of Chemistry of High-purity Substances of RAS in Nizhniy Novgorod, and also M. F. Churbanov MRAS and his coworkers P. G. Sennikov, A. D. Bulanov and

A. V. Gusev for their commitment, fundamental work and punctual delivery of the enriched material. The support of the project with advice and funds from our directors and the daily work of our colleagues for the results reached thus far are warmly acknowledged.

References

[1] P. Becker, Rep. Prog. Phys. **64**, 1945 (2001).
[2] R. L. Steiner, E. R. Williams, and D. B. Newell, Metrologia **42**, 431 (2005).
[3] P. Becker, P. DeBièvre, K. Fujii, M. Gläser, B. Inglis, H. Lübbig, and G. Mana, Metrologia **44**, 1 (2007).
[4] Yu. V. Tarbeyev, A. K. Kaliteevski, V. I. Sergeyev, R. D. Smirno, and O. N. Godisov, Metrologia **31**, 269 (1994).
[5] P. Becker, F. Spieweck, H. Bettin, U. Kuetgens, J. Stümpel, P. DeBievre, S. Valkiers, W. Zulehner, and C. Holm, IEEE Trans. Instrum. Meas. **44**, 5282 (1995).
[6] P. Becker, H. Friedrich, K. Fujii, G. Mana, H.-J. Pohl, H. Riemann, and S. Valkiers, Meas. Sci. Technol. MST **20**, 092002 (20pp) (2009).
[7] M. Cardona and M. L. W. Thewalt, Rev. Mod. Phys. **77**, 1173 (2005).
[8] A. Yang, M. Steger, D. Karaisky, M. L. W. Thewalt, M. Cardona, K. M. Itoh, H. Riemann, N. V. Abrosimov, M. F. Churbanov, A. V. Gusev, A. D. Bulanov, A. K. Kaliteevskii, O. N. Godisov, P. Becker, H.-J. Pohl, J. W. Ager, and E. E. Haller, Phys. Rev. Lett. **97**, 227401 (2006).
[9] D. Karaiskaj, M. L. W. Thewalt, T. Ruf, M. Cardona, H.-J. Pohl, G. G. Deviatych, P. G. Sennikov, and H. Riemann, Phys. Rev. Lett. **86**, 6010 (2001).
[10] K. M. Itoh, Solid State Commun. **133**, 747 (2005).
[11] T. D. Ladd, D. Maryenko, Y. Yamamoto, E. Abe, and K. M. Itoh, Phys. Rev. B **71**, 014401 (2005).
[12] Y. Shimizu, M. Uematsu, K. M. Itoh, A. Taksano, K. Sawano, and Y. Shyraki, Appl. Surf. Sci. **255**, 1345 (2008).
[13] Y. Shimizu, M. Uematsu, K. M. Itoh, A. Taksano, K. Sawano, and Y. Shyraki, Appl. Phys. Express **1**, 021401 (2006).
[14] D. Bulanov, G. G. Devyatych, A. V. Gussev, P. G. Sennikov, H.-J. Pohl, H. Riemann, H. Schilling, and P. Becker, Cryst. Res. Technol. **35**, 1023 (2000).
[15] J. Gebauer, F. Rudolf, A. Polity, R. Krause-Rehberg, J. Martin, and P. Becker, Appl. Phys. A **68**, 411 (1999).
[16] T. Steinegger, M. Naumann, F. Kirscht, Solid State Phenom. **108/109**, 597 (2005).
[17] N. V. Abrosimov, H. Riemann, H.-J. Pohl, A. K. Kalitevski, O. N. Godisov, V. A. Korolyov, and A. J. Zhilnikov, J. Cryst. growth, Cryst. Res. Technol. **7/8**, 654-658 (2003) /10.1002/crat.200310064.
[18] P. Becker, D. Schiel, H.-J. Pohl, A. K. Kaliteevski, O. N. Godisov, M. F. Churbanov, G. G. Devyatykh, A. V. Gusev, A. D. Bulanov, S. A. Adamchik, V. A. Gavva, I. D. Kovalev, N. V. Abrosimov, B. Hallmann-Seiffert, H. Riemann, S. Valkiers, P. Taylor, P. DeBièvre, and E. M. Dianov, J. Meas. Sci. Technol. **21**, 1854 (2006).
[19] H.-J. Pohl and P. DeBièvre, Technical Road Map for the Production of ^{28}Si Single Crystal Precursors for ^{28}Si AVOGADRO Spheres (TRM28), Laboratory Report Physikalisch-Technische Bundesanstalt Braunschweig (2005).
[20] E. I. Abbakumov, V. A. Bazhenov, Ju. V. Verbin, A. A. Vlasov, A. S. Dorogobed, A. K. Kaliteevski, V. F. Kornilov, D. M. Levin, E. I. Mikerin, A. A. Sazykin, V. I. Sergejev, and G. S. Solovjev, Atomnaya Energiya **67**, 255 (1989).
[21] A. L. Kaliteevski, O. N. Godisov, and A. Yu. Safronov, Elaboration of the complex of technologies and obtaining of superclean and high enriched Silicon 28 isotope for International Project of an improvement of an Avogadro constant, X. Int. Sci. Conf. Phys. Chem. Proc. at selection of Atoms and molecules, Zvenigorod,/Mov. 3–8, 10 (2005).
[22] G. G. Devyatych, A. D. Bulanov, A. V. Gusev, I. D. Kovalev, V. A. Krylov, A. M. Potapov, P. G. Sennikov, S. A. Adamchik, V. A. Gavra, A. P. Kotkov, M. F. Churbanov, E. M. Dianov, A. K. Kaliteevski, O. N. Godisov, H. J. Pohl, P. Becker, H. Rieman, and N. Y. Abrosimov, Dokl. Chemistry RAN 0012-5008, Vol. 421, part1, Nos 1–3, p. 151 (2008).
[23] K. Fujii, A. Waseda, N. Kuramoto, S. Mizushima, P. Becker, H. Bettin, A. Nicolaus, U. Kuetgens, S. Valkiers, P. Taylor, P. DeBievre, G. Mana, G. Massa, R. Matyi, E. G. Kessler, and M. Hamke, IEEE Trans. Instrum. Meas. **54**, 854 (2005).
[24] R. A. Nicolaus and G. Bönsch, IEEE Trans. Instrum. Meas. **46**, 563 (1997).
[25] A. Yang, M. Steger, D. Karaisky, M. L. W. Thewalt, M. Cardona, K. M. Itoh, H. Riemann, N. V. Abrosimov, M. F. Churbanov, A. V. Gusev, A. D. Bulanov, A. K. Kaliteevskii, O. N. Godisov, P. Becker, H.-J. Pohl, J. W. Ager, and E. E. Haller, Phys. Rev. Lett. **97**, 227401 (2006).
[26] M. L. W. Thewalt, A. Yang, M. Steger, D. Karaisky, M. Cardona, H. Riemann, N. V. Abrosimov, A. V. Gusev, A. D. Bulanov, I. D. Kovalev, A. K. Kaliteevski, O. N. Godisov, P. Becker, H.-J. Pohl, E. E. Haller, J. W. Ager, III, and K. M. Itoh, Appl. Phys. **101**, 081724 (2007).
[27] M. Steger, A. Yang, D. Karaisky, M. L. W. Thewalt, E. E. Haller, J. W. Ager , III, M. Cardona, H. Riemann, N. V. Abrosimov, A. V. Gusev, A. D. Bulanov, A. K. Kaliteevski, O. N. Godisov, P. Becker, and H.-J. Pohl, Shallow impurity IR-Absorption Spectroscopy in Isotopical enriched Silicon, Proceedings ICPS 2006, Vienna, Austria, July 24–28, 2006, p. 600.
[28] M. Steger, A. Yang, M. L. W. Thewalt, M. Cardona, H. Riemann, N. V. Abrosimov, M. F. Churbanov, A. V. Gusev, A. D. Bulanov, I. D. Kovalev, A. K. Kaliteevski, O. N. Godisov, P. Becker, H.-J. Pohl, J. W. Ager, III, and E. E. Haller, Physica B **391**, 402 (2007).
[29] M. L. W. Thewalt, M. Steger, A. Yang, M. Cardona, H. Riemann, N. V. Abrosimov, M. F. Churbanov, A. V. Gusev, A. D. Bulanov, I. D. Kovalev, A. K. Kaliteevski, O. N. Godisov, P. Becker, and H.-J. Pohl, Well-resolved Hyperfine Structure in the Absorption Spectrum of ^{27}Se in High Enriched ^{28}Si, Proceedings ICPS 2006 Vienna, Austria, July 24–28, 2006, p. 435.
[30] A. Yang, M. Steger, T. Sekiguchi, M. L. W. Thewalt, T. D. Ladd, K. M. Itoh, H. Riemann, N. Abrosimov, P. Becker, and H.-J. Pohl, Phys. Rev. Lett. **102**, 257401 (2009).
[31] M. Kohei and K. M. Itoh, Solid State Commun. **133**, 747 (2005).
[32] T. D. Ladd, D. Maryenko, Y. Yamamoto, E. Abe, and K. M. Itoh, Phys. Rev. B **71**, 014401 (2005).
[33] T. D. Ladd, D. Maryenko, Y. Yamamoto, E. Abe, and K. M. Itoh, Coherence time of solid state nuclear qubit, arxiv qquant-üh/0309164v1 23.11.2003.

[34] T. Ruf, R. W. Henn, M. Asen-Palmer, E. Gmelin, M. Cardona, H.-J. Pohl, G. G. Devyatych, and P. G. Sennikov, Solid State Commun. **116**, 243 (2000).
[35] R. K. Kremer, A. Graf, M. Cardona, G. G. Devyatych, A. V. Gusev, A. M. Gibin, A. V. Inyushkin, A. N. Taldenko, and H.-J. Pohl, Solid State Commun. **131**, 499 (2004).
[36] T. Kojima, R. Nebashi, K. M. Itoh, and Y. Shiraki, Appl. Phys. Lett. **38**, 2318 (1977).
[37] P. G. Baranov, B. Ya. Ber, O. N. Godisov, I. V. Ilyin, A. N. Yaonov, A. K. Laöiteevski, M. A. Kaliteevski, I. M. Lazebnik, P. C. Kopyev, H. Riemann, and N. V. Abrosimov, Proceedings 7th Russ. Conf. on Physics of Semiconductors (2005).
[38] I. C. Kizilyalli, S. J. Burden, H. Safar, and P. L. Gammel, IEEE Electron Device Lett. **26**, 404 (2005).
[39] G. Albrecht, G. G. Devyatych, J. Osten, and P.-G. Sennikov, private communication (2000).
[40] Y. Shimizu, M. Uematsu, M. Kohei, K. M. Itoh, A. Takano, K. Sawano, and Y. Shiraki, Appl. Phys. Express **1**, 021401 (2008).
[41] P. G. Sennikov, S. V. Golubev, V. I. Schaschkin, D. A. Pryakhin, M. N. Drozdov, B. A. Andreev, H. J. Pohl, and O. N. Godisov, J. Tech. Phys. Lett. **35**, 41 (2009) (in Russian).
[42] N. Abosimov, P. Sennikov, and H.-J. Pohl, 2009, private communication.

